Set-Valued Estimation of Freeway Traffic Density

Alex A. Kurzhanskiy

University of California, Berkeley, CA 94720-1770, United States
(e-mail: akurzhan@eecs.berkeley.edu)

Abstract: The information about traffic density on a freeway is required by real time traffic responsive ramp flow controllers. Currently, density cannot be measured directly and has to be estimated from traffic flow and/or velocity measurements.
This paper describes the algorithm for the set-valued density estimation using the macroscopic first order Cell Transmission Model (CTM) together with combined flow and velocity measurements. It is assumed that freeway cell capacities, on-ramp demands and measurement noise values are not known exactly, but lie within certain intervals. Monotonicity of CTM allows to reduce density estimation to a series of interval arithmetic operations.

Keywords: set-valued estimation, interval analysis, cell transmission model, uncertain fundamental diagram, monotone system

1. INTRODUCTION

Traffic responsive ramp flow control algorithms use freeway traffic density as feedback. Currently deployed technologies (loop detectors, probes) cannot measure density directly, but obtain quantities (traffic flow and velocity) from which density can be derived.

This paper [1] shows how macroscopic Cell Transmission Model (CTM) [1] with uncertainty in fundamental diagrams and demands can be used in combination with periodic noisy flow and velocity measurements to estimate the density. Uncertainties and noise in each cell lie within intervals whose bounds are known functions of time. Monotonicity of the CTM [2] allows to compute box bounds for the density at each time using simple interval arithmetic.

In the rest of the paper Section 2 describes CTM and its properties; Section 3 explores CTM observability in a 2-cell example; Section 4 sets the problem; Section 5 presents the estimation algorithm; Section 6 shows application of this algorithm to I-210 West freeway in Southern California; Appendix A contains some facts about the interval arithmetic.

2. CTM AND ITS PROPERTIES

The freeway is divided into N cells, each with one on- and one off-ramp, indexed $1..N$, shown in Fig. 1. Cell i is upstream of cell $i+1$. Free flow prevails downstream of cell N; upstream of the freeway is the inflow of r_0. The flow accepted by cell 1 is $f_0(t)$ vehicles per hour. Cell

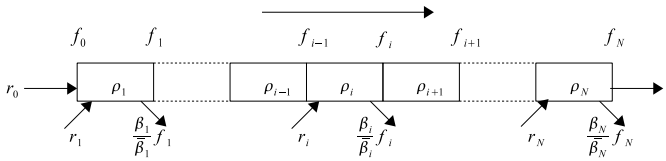

Fig. 1. Freeway divided into N cells.

i is characterized by a single state variable, its density ρ_i, so the state of the freeway is the N-dimensional vector $\rho = (\rho_1, \cdots, \rho_N)$. Vehicle movement in a cell is governed by a triangular fundamental diagram defined by capacity, free flow speed and congestion wave speed. (Fig. 2). Density value that corresponds to the capacity is the

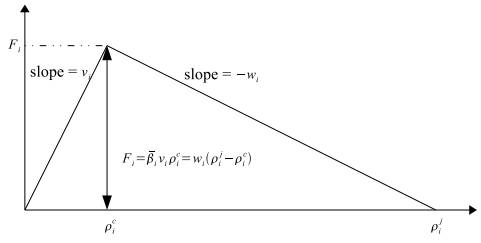

Fig. 2. Fundamental diagram in cell i.

critical density, and density at which the traffic speed is 0 is the jam density. The state of a freeway obeys a N-dimensional nonlinear differential equation.

$$\dot{\rho}_i(t) = \frac{1}{l_i}\left(f_{i-1}(t) - \frac{f_i(t)}{\bar{\beta}_i(t)} + r_i(t)\right),\ i = 1..N, \qquad (1)$$

with

$$f_0(t) = \min\left\{r_0(t),\ w_1(\rho_1^j - \rho_1(t)),\ F_1\right\}, \qquad (2)$$

$$f_i(t) = \min\left\{v_i\rho_i(t),\ w_{i+1}(\rho_{i+1}^j - \rho_{i+1}(t)),\ F_{i+1}\right\}, \qquad (3)$$

$$f_N(t) = \min\left\{v_N\rho_N(t),\ F_N\right\}, \qquad (4)$$

[1] This research is conducted within the TOPL project, that is supported by the California Department of Transportation through the California PATH program.

where N is the number of cells; i is the cell index (in 3 $i = 1..N-1$); l_i is the length of cell i in *miles*; t is the time; ρ_i^c is the critical density for cell i, in *vehicles per mile*; ρ_i^j is the jam density for cell i, in *vehicles per mile*; F_i is the capacity of cell i, in *vehicles per hour*; $v_i = \frac{F_i}{\rho_i^c}$ is the free flow speed, in *miles per hour*; $w_i = \frac{F_i}{\rho_i^j - \rho_i^c}$ is the congestion wave speed, in *miles per hour*; $\rho_i(t)$ is the density in cell i, in *vehicles per mile*; $\rho(t)$ is the N-dimensional vector of densities; $f_0(t)$ is the flow entering the first cell in *vehicles per hour*; $f_i(t)$ is the flow leaving cell i, in *vehicles per hour*; $r_0(t)$ is the mainline demand, in *vehicles per hour*; $r_i(t)$ is the on-ramp demand for cell i, in *vehicles per hour*; $\beta_i(t)$ is the off-ramp split ratio for cell i, $0 \le \beta_i(t) \le 1$, defines which portion of the cell outflow leaves through the off-ramp; $\bar{\beta}_i(t) = 1 - \beta_i(t)$ is the complementary split ratio for cell i.

It was shown in [2] that system (1)-(4) is monotone — for any initial conditions $\tilde{\rho}(0)$ and $\hat{\rho}(0)$, such that $\tilde{\rho}(0) < \hat{\rho}(0)$, it is true that $\tilde{\rho}(t) < \hat{\rho}(t)$ for any $t \ge 0$ [2].

The goal is to estimate the state $\rho(t)$. Measurement data comes from point and/ or mobile sensors. Point sensors measure flows $f_i(t)$, and mobile sensors measure traffic velocities $V_i(t)$, $i = 1..N$, inside the cells. For cell i, density $\rho_i(t)$, flow $f_i(t)$ and velocity $V_i(t)$ are related as

$$V_i(t) = \frac{f_i(t)}{\bar{\beta}_i \rho_i(t)}. \tag{5}$$

The measurement can be either N-dimensional vector flows $y_f(t)$ in the case of point sensors, or N-dimensional vector of velocities $y_V(t)$ in the case of mobile sensors. Specifically,

$$y_f(t) = \begin{pmatrix} f_1(t) \\ \vdots \\ f_N(t) \end{pmatrix}, \tag{6}$$

and

$$y_V(t) = \begin{pmatrix} f_1(t)/\bar{\beta}_1 \rho_1(t) \\ \vdots \\ f_N(t)/\bar{\beta}_N \rho_N(t)) \end{pmatrix}. \tag{7}$$

Proposition 1. System (1)-(4) is completely observable
1. under flow measurement $y_f(t)$ iff all cells are in free flow:

$$f_0(t) = r_0 \text{ and } f_i(t) = v_i \rho_i(t),\ i = 1..N,$$

or all cells are congested and the mainline demand r_0 cannot be satisfied:

$$f_i(t) = w_{i+1}(\rho_{i+1}^j - \rho_{i+1}(t)),\ i = 0..N-1,$$
$$f_N(t) = F_N,$$

or upstream cells are congested, the mainline demand r_0 cannot be satisfied and free flow cells can only be downstream of the congested cells:

$$f_i(t) = w_{i+1}(\rho_{i+1}^j - \rho_{i+1}(t)),\ i = 0..M-1 < N-1,$$
$$f_i(t) = v_i \rho_i(t),\ i = M+1..N;$$

[2] For two vectors $x, y \in \mathbf{R}^N$, $x \le y \Leftrightarrow x_i \le y_i$, $i = 1..N$, and $x < y \Leftrightarrow x \le y$, $x \ne y$.

2. under velocity measurement $y_V(t)$ iff all cells are congested:

$$f_i(t) = w_{i+1}(\rho_{i+1}^j - \rho_{i+1}(t)),\ i = 1..N-1,$$
$$f_N(t) = F_N.$$

To get a better understanding of this proposition, consider the simple 2-cell example.

3. EXAMPLE: 2-CELL FREEWAY SEGMENT

Consider freeway segment shown in Fig. 3 with the following parameters: $l_1 = l_2 = 1$ mile; $\rho_1^c = \rho_2^c = \rho^c = 100$ vpm; $\rho_1^j = \rho_2^j = \rho^j = 400$ vpm; $F_1 = F_2 = F = 6000$ vph; $v_1 = v_2 = v = \frac{F}{\rho^c} = 60$ mph; $w_1 = w_2 = w = \frac{F}{\rho^j - \rho^c} = 20$ mph; $r_0 = 4800$ vph; and $r_2 = 1200$ vph.

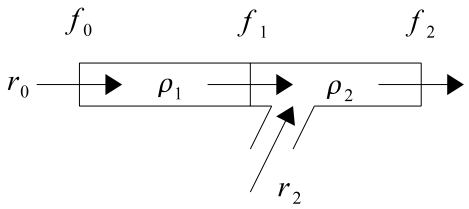

Fig. 3. 2-cell example.

Piecewise affine system (1)-(4) for $N = 2$ has six affine modes listed in Table 1.

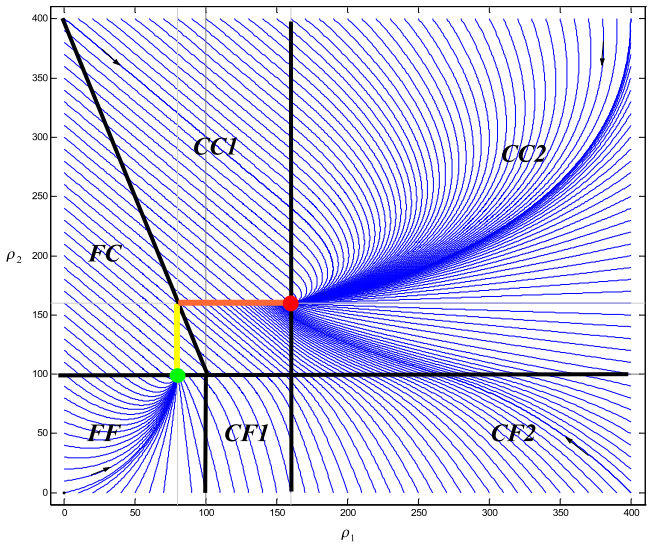

Fig. 4. Phase portrait of the 2-cell system and the partition into regions with affine dynamics. Green and red dots together with yellow and orange line segments depict the set of equilibria for this system.

Fig. 4 illustrates the dynamics of the 2-cell system and shows how the state space is partitioned into six regions *FF*, *FC*, *CF1*, *CF2*, *CC1* and *CC2*, in each of which the system dynamics is affine and the observation equation

Mode	Conditions	System Equations
FF	$\rho_1(t) \le \rho_1^c$ $\rho_2(t) \le \rho_2^c$	$\dot{\rho}(t) = \begin{pmatrix} -v_1 & 0 \\ v_1 & -v_2 \end{pmatrix} \rho(t) + \begin{pmatrix} r_0 \\ r_2 \end{pmatrix}$ $y_f(t) = \begin{pmatrix} v_1 & 0 \\ 0 & v_2 \end{pmatrix} \rho(t)$ $y_V(t) = \begin{pmatrix} v_1 \\ v_2 \end{pmatrix}$
FC	$v_1\rho_1(t) \le w_2(\rho_2^j - \rho_2(t))$ $\rho_2(t) > \rho_2^c$	$\dot{\rho}(t) = \begin{pmatrix} -v_1 & 0 \\ v_1 & 0 \end{pmatrix} \rho(t) + \begin{pmatrix} r_0 \\ r_2 - F_2 \end{pmatrix}$ $y_f(t) = \begin{pmatrix} v_1 & 0 \\ 0 & 0 \end{pmatrix} \rho(t) + \begin{pmatrix} 0 \\ F_2 \end{pmatrix}$ $y_V(t) = \begin{pmatrix} v_1 \\ F_2/\rho_2(t) \end{pmatrix}$
CF1	$\rho_1(t) > \rho_1^c$ $w_1(\rho_1^j - \rho_1(t)) \ge r_0$ $\rho_2(t) \le \rho_2^c$	$\dot{\rho}(t) = \begin{pmatrix} 0 & 0 \\ 0 & v_2 \end{pmatrix} \rho(t) + \begin{pmatrix} r_0 - F_2 \\ r_2 \end{pmatrix}$ $y_f(t) = \begin{pmatrix} 0 & 0 \\ 0 & v_2 \end{pmatrix} \rho(t) + \begin{pmatrix} F_2 \\ 0 \end{pmatrix}$ $y_V(t) = \begin{pmatrix} F_2/\rho_1(t) \\ v_2 \end{pmatrix}$
CF2	$w_1(\rho_1^j - \rho_1(t)) < r_0$ $\rho_2(t) \le \rho_2^c$	$\dot{\rho}(t) = \begin{pmatrix} -w_1 & 0 \\ 0 & v_2 \end{pmatrix} \rho(t) + \begin{pmatrix} w_1\rho_1^j - F_2 \\ r_2 \end{pmatrix}$ $y_f(t) = \begin{pmatrix} -w_1 & 0 \\ 0 & v_2 \end{pmatrix} \rho(t) + \begin{pmatrix} w_1\rho_1^j - F_2 \\ 0 \end{pmatrix}$ $y_V(t) = \begin{pmatrix} F_2/\rho_1(t) \\ v_2 \end{pmatrix}$
CC1	$w_2(\rho_2^j - \rho_2(t)) < v_1\rho_1(t)$ $w_1(\rho_1^j - \rho_1(t)) \ge r_0$ $\rho_2(t) > \rho_2^c$	$\dot{\rho}(t) = \begin{pmatrix} 0 & w_2 \\ 0 & -w_2 \end{pmatrix} \rho(t) + \begin{pmatrix} r_0 - w_2\rho_2^j \\ w_2\rho_2^j + r_2 - F_2 \end{pmatrix}$ $y_f(t) = \begin{pmatrix} 0 & -w_2 \\ 0 & 0 \end{pmatrix} \rho(t) + \begin{pmatrix} 0 \\ F_2 \end{pmatrix}$ $y_V(t) = \begin{pmatrix} w_2(\rho_2^j - \rho_2(t))/\rho_1(t) \\ F_2/\rho_2(t) \end{pmatrix}$
CC2	$w_1(\rho_1^j - \rho_1(t)) < r_0$ $\rho_2(t) > \rho_2^c$	$\dot{\rho}(t) = \begin{pmatrix} -w_1 & w_2 \\ 0 & -w_2 \end{pmatrix} \rho(t) + \begin{pmatrix} 0 \\ w_2\rho_2^j + r_2 - F_2 \end{pmatrix}$ $y_f(t) = \begin{pmatrix} -w_1 & 0 \\ 0 & -w_2 \end{pmatrix} \rho(t) + \begin{pmatrix} w_1\rho_1^j \\ w_2\rho_2^j \end{pmatrix}$ $y_V(t) = \begin{pmatrix} w_2(\rho_2^j - \rho_2(t))/\rho_1(t) \\ F_2/\rho_2(t) \end{pmatrix}$

Table 1. System (1)-(4), with observation equations for the 2-cell example.

for $y_f(t)$ is affine[3]. From the observation equations in Table 1 it is easy to see which part of the state $\rho(t)$ can be determined from which measurements in each affine mode. The question of observability of the CTM system as a whole is more complex, as we need to determine the affine mode in the first place. Under flow measurement the affine mode can be uniquely determined if it is *FF*, *CC2*, *CF2* or *CF1*. On the other hand, it is impossible to distinguish between modes *FC* and *CC1*. This fact is illustrated in Fig. 4, which shows the set of equilibria of the system, and in each equilibrium state the measured flows are the same. Under velocity measurement the affine mode can always be determined.

Table 2 summarizes the observability properties of the 2-cell system in each affine mode. Apparently, measuring the flow $y_f(t)$ is sufficient for estimating the density only in the modes *FF*, *CC2* and *CF2*. The system is unobservable in *CF1* and, obviously, in *FC* and *CC1*. At the same time, measuring velocity $y_V(t)$ is sufficient for estimating the density only in modes *CC1* and *CC2*, where the speed is below free flow in all cells. In modes *FC* and *CF1* it is not enough to measure just flow or just velocity to determine density $\rho(t)$ — here we need both measurements, $y_f(t)$ and $y_V(t)$. Recall Proposition 1.

In [5] the authors investigate the observability of CTM for the case of flow measurement and argue that using piecewise affine approximation of the original system with just two affine modes, which correspond to our *FF* and *CC2* switching randomly between those, is fair enough for the purpose of density estimation. The obvious setback of this approach is that such approximation of CTM is no longer a conservation law and thus has different dynamics. The reason why estimation with the two-mode switching model produces decent results is in the fact that the demand is practically never feasible — it is either strictly feasible or infeasible. It was shown in [2] that for both, strictly feasible and infeasible demand, the system has globally asymptotically stable equlibrium points, and thus, it has to end up in either all free flow *FF* or all congested *CC2* mode, while other modes are transient.

[3] The number of affine modes grows exponentially with the dimension of the system. For general N the number of affine modes is $2^N + 2$.

Mode	Flow measurement $y_f(t)$	Velocity measurement $y_V(t)$
FF	$\rho_1(t)$ – observable	$\rho_1(t)$ – unobservable
	$\rho_2(t)$ – observable	$\rho_2(t)$ – unobservable
FC	$\rho_1(t)$ – observable	$\rho_1(t)$ – unobservable
	$\rho_2(t)$ – unobservable	$\rho_2(t)$ – observable
CF1	$\rho_1(t)$ – unobservable	$\rho_1(t)$ – observable
	$\rho_2(t)$ – observable	$\rho_2(t)$ – unobservable
CF2	$\rho_1(t)$ – observable	$\rho_1(t)$ – observable
	$\rho_2(t)$ – observable	$\rho_2(t)$ – unobservable
CC1	$\rho_1(t)$ – unobservable	$\rho_1(t)$ – observable
	$\rho_2(t)$ – observable	$\rho_2(t)$ – observable
CC2	$\rho_1(t)$ – observable	$\rho_1(t)$ – observable
	$\rho_2(t)$ – observable	$\rho_2(t)$ – observable

Table 2. Observability of the 2-cell system.

4. PROBLEM SETTING

Assume that cell lengths l_i, free flow speeds v_i, congestion propagation speeds w_i and split ratios $\beta_i(t)$, $i = 1..N$, are the exactly known parameters of system (1)-(4); demands $r_i(t)$ are known with some uncertainty, more precisely, they are constrained by a box $r_i^-(t) \le r_i(t) \le r_i^+(t)$ ($r_i^-(t)$ and $r_i^+(t)$ are known), $i = 0..N$ [4]; cell capacities F_i lie within given intervals $F_i^- \le F_i \le F_i^+$ (F_i^- and F_i^+ are known), $i = 1..N$. Accordingly, denote

$$\rho_i^{j+} = \frac{F_i^+}{w_i} + \frac{F_i^+}{v_i} \quad \text{and} \quad \rho_i^{j-} = \frac{F_i^-}{w_i} + \frac{F_i^-}{v_i}. \tag{8}$$

Measurement noise $\omega(t)$ is present and is bounded by given box-valued constraint. So, the observation equation is

$$y(t) = h(t, \rho(t)) + \omega(t), \tag{9}$$

Where $h(t, \rho(t))$ is specific for $y_f(t)$ and $y_V(t)$.

To ensure complete observability of the system, both, flow measurment $y_f(t)$ and velocity measurement $y_V(t)$ must be available [5]. The state estimation for the system (1)-(4), (9) is performed with $y(t) = \begin{pmatrix} y_f(t) \\ y_V(t) \end{pmatrix}$, and

$$\omega_f(t) \in \left\{\bar\omega_f \in \mathbf{R}^N \middle| -\omega_{fi}^0(t) \le \bar\omega_{fi} \le \omega_{fi}^0(t), i = 1..N\right\}, \tag{10}$$

$$\omega_V(t) \in \left\{\bar\omega_V \in \mathbf{R}^N \middle| -\omega_{Vi}^0(t) \le \bar\omega_{Vi} \le \omega_{Vi}^0(t), i = 1..N\right\}, \tag{11}$$

where subscript $_f$ indicates values related to flow measurements, subscript $_V$ indicates values related to velocity measurements, and $\omega_f^0(t) = \begin{pmatrix} \omega_{f1}^0(t) \\ \vdots \\ \omega_{fN}^0(t) \end{pmatrix}$, $\omega_V^0(t) = \begin{pmatrix} \omega_{V1}^0(t) \\ \vdots \\ \omega_{VN}^0(t) \end{pmatrix}$, $0 \le t$, are known nonnegative functions.

[4] The problem of demand prediction can be addressed by various available approaches, such as [4, 6, 8]. Systems such as PeMS [7] provide historic measurement data.

[5] Had there be no noise ($\omega(t) = 0$), we could determine density $\rho(t)$ without using the state equation (1)-(4), only from the measurements $y_f(t)$ and $y_V(t)$ and formula (5): $\rho_i(t) = y_{fi}(t)/\bar\beta_i y_{Vi}(t)$, $i = 1..N$. In reality, however, the noise is present.

5. SET-VALUED ESTIMATION

Define state equations

$$\dot\rho_i^-(t) = \frac{1}{l_i}\left(f_{i-1}^-(t) - \frac{f_i^+(t)}{\bar\beta_i(t)} + r_i^-(t)\right), \ i = 1..N, \quad (1^-)$$

and

$$\dot\rho_i^+(t) = \frac{1}{l_i}\left(f_{i-1}^+(t) - \frac{f_i^-(t)}{\bar\beta_i(t)} + r_i^+(t)\right), \ i = 1..N, \quad (1^+)$$

where

$$f_0^-(t) = \min\left\{r_0^-(t),\ w_1(\rho_1^{j-} - \rho_1^+(t)),\ F_1^-\right\}, \quad (2^-)$$

$$f_0^+(t) = \min\left\{r_0^+(t),\ w_1(\rho_1^{j+} - \rho_1^-(t)),\ F_1^+\right\}, \quad (2^+)$$

$$f_i^-(t) = \min\left\{v_i\rho_i^-(t), w_{i+1}(\rho_{i+1}^{j-} - \rho_{i+1}^+(t)), F_{i+1}^-\right\}, \quad (3^-)$$

$$f_i^+(t) = \min\left\{v_i\rho_i^+(t), w_{i+1}(\rho_{i+1}^{j+} - \rho_{i+1}^-(t)), F_{i+1}^+\right\}, \quad (3^+)$$

for $i = 1..N-1$,

$$f_N^-(t) = \min\left\{v_N\rho_N^-(t),\ F_N^-\right\}. \quad (4^-)$$

$$f_N^+(t) = \min\left\{v_N\rho_N^+(t),\ F_N^+\right\}. \quad (4^+)$$

Remark. Note that in (2^-) and (3^-), it may happen that $\rho_i^+(t) > \rho_i^{j-}$. Therefore, one has to ensure that $f_i^-(t) \ge 0$ by setting $f_i^-(t) = \max\{f_i^-(t), 0\}$, $i = 1..N$.

Due to monotonicity of (1)-(4) and the fact that $f_i^+(t) \ge f_i^-(t)$ and $r_i^+(t) \ge r_i^-(t)$, $i = 0..N$, for initial conditions $\rho^-(0) \le \rho(0) \le \rho^+(0)$, it is true that

$$\rho^-(t) \le \rho(t) \le \rho^+(t), \quad t \ge 0, \tag{12}$$

where $\rho(\cdot)$ is trajectory of (1)-(4), $\rho^-(\cdot)$ is trajectory of (1^-)-(4^-), and $\rho^+(\cdot)$ is trajectory of (1^+)-(4^+).

Data measurements are collected at times $0 = \tau_0 < \tau_1 < \cdots < \tau_{K-1} < \tau_K = T$, where T is some termination time. The state estimation algorithm works as follows.

1. First, compute the initial conditions — that is, determine bounds for the initial state $\rho(0)$. At time $t = 0$ take the first measurement $y(0) = \begin{pmatrix} y_f(0) \\ y_V(0) \end{pmatrix}$, which together with (9) gives us

$$\hat\rho(0) = \begin{pmatrix} \dfrac{y_{f1}(0) - \omega_{f1}(0)}{\bar\beta_1(y_{V1}(0) - \omega_{V1}(0))} \\ \vdots \\ \dfrac{y_{fN}(0) - \omega_{fN}(0)}{\bar\beta_N(y_{VN}(0) - \omega_{VN}(0))} \end{pmatrix},$$

where $\omega_{fi}(0)$, $\omega_{Vi}(0)$, $i = 1..N$, are known each within interval $\omega_{fi}(0) \in [-\omega_{fi}^0(0), \omega_{fi}^0(0)]$ and $\omega_{Vi}(0) \in [-\omega_{Vi}^0(0), \omega_{Vi}^0(0)]$. So,

$$\hat\rho_i(0) \in [\hat\rho_i^-(0), \hat\rho_i^+(0)], \quad i = 1..N. \tag{13}$$

Suppose, the following conditions hold:

$$y_{fi}(0) - \omega_{fi}^0(0) > 0, \tag{14}$$

and

$$y_{Vi}(0) - \omega_{Vi}^0(0) > 0. \tag{15}$$

Then, following (A.1) and (A.9) from Appendix A, we get

$$\hat{\rho}_i^-(0) = \frac{y_{fi}(0) - \omega_{fi}^0(0)}{\bar{\beta}_i(y_{Vi}(0) + \omega_{Vi}^0(0))} \quad (16)$$

$$\hat{\rho}_i^+(0) = \frac{y_{fi}(0) + \omega_{fi}^0(0)}{\bar{\beta}_i(y_{Vi}(0) - \omega_{Vi}^0(0))}. \quad (17)$$

If condition (15) does not hold, set

$$\hat{\rho}_i^-(0) = \rho_i^{j-} \text{ and } \hat{\rho}_i^+(0) = \rho_i^{j+}, \quad (18)$$

where ρ_i^{j-} and ρ_i^{j+} are defined in (8); and if condition (15) holds but condition (14) does not, set

$$\hat{\rho}_i^-(0) = \hat{\rho}_i^+(0) = 0. \quad (19)$$

There may be some apriori knowledge about the bounds of the initial state [6]:

$$\rho_i(0) \in [\rho_i^-(0), \rho_i^+(0)], \quad i = 1..N, \quad (20)$$

then, the initial state should belong to the intersection of sets (13) and (20):

$$\Big\{\rho \in \mathbf{R}_+^N \mid \rho_i \in [\rho_i^-(0), \rho_i^+(0)] \cap [\hat{\rho}_i^-(0), \hat{\rho}_i^+(0)],\ i = 1..N\Big\}. \quad (21)$$

If this set is not empty, update the initial state bounds:

$$\underline{\rho}_i(0) = \max(\rho_i^-(0), \hat{\rho}_i^-(0)), \quad (22)$$

$$\overline{\rho}_i(0) = \min(\rho_i^+(0), \hat{\rho}_i^+(0)), \quad (23)$$

else, if (21) is empty, or there is no apriori information about the initial state, set

$$\underline{\rho}_i(0) = \min(\hat{\rho}_i^-(0), \rho_i^{j-}), \quad (24)$$

$$\overline{\rho}_i(0) = \min(\hat{\rho}_i^+(0), \rho_i^{j+}) \quad (25)$$

for $i = 1..N$.
The initial state estimate is

$$\underline{\rho}(0) \le \rho(0) \le \overline{\rho}(0).$$

Now, for $k = 1..K$ repeat the following steps.

2. Given the initial conditions $\rho^-(\tau_{k-1}) = \underline{\rho}(\tau_{k-1})$ and $\rho^+(\tau_{k-1}) = \overline{\rho}(\tau_{k-1})$, compute trajectories $\rho^-(t)$ and $\rho^+(t)$, $\tau_{k-1} \le t \le \tau_k$.
If $\underline{\rho}(\tau_{k-1}) \le \rho(\tau_{k-1}) \le \overline{\rho}(\tau_{k-1})$, then following (12) we get

$$\rho(t) \in \big\{\rho \in \mathbf{R}_+^N \mid \rho_i^-(t) \le \rho_i \le \rho_i^+(t),\ i = 1..N\big\} \quad (26)$$

for $t \in [\tau_{k-1}, \tau_k)$.

3. At time $t = \tau_k$ the measurement $y(\tau_k) = \begin{pmatrix} y_f(\tau_k) \\ y_V(\tau_k) \end{pmatrix}$ is received. As in step **1**, it gives the estimate

$$\hat{\rho}(\tau_k) \in \big\{\hat{\rho} \in \mathbf{R}_+^N \mid \hat{\rho}_i^-(\tau_k) \le \hat{\rho}(\tau_k) \le \hat{\rho}_i^+(\tau_k),\ i = 1..N\big\}, \quad (27)$$

where

$$\hat{\rho}_i^-(\tau_j) = \frac{y_{fi}(\tau_k) - \omega_{fi}^0(\tau_k)}{\bar{\beta}_i(y_{Vi}(\tau_k) + \omega_{Vi}^0(\tau_k))} \quad (28)$$

$$\hat{\rho}_i^+(\tau_k) = \frac{y_{fi}(\tau_k) + \omega_{fi}^0(\tau_k)}{\bar{\beta}_i(y_{Vi}(\tau_k) - \omega_{Vi}^0(\tau_k))} \quad (29)$$

if conditions

$$\hat{y}_{fi}(\tau_k) - \omega_{fi}^0(\tau_k) > 0 \quad (30)$$

and

$$\hat{y}_{Vi}(\tau_k) - \omega_{Vi}^0(\tau_k) > 0 \quad (31)$$

are satisfied.
Otherwise, if condition (31) does not hold, set

$$\hat{\rho}_i^-(\tau_k) = \rho_i^{j-} \text{ and } \hat{\rho}_i^+(\tau_k) = \rho_i^{j+}, \quad (32)$$

or, if (31) holds, but (30) does not, set

$$\hat{\rho}_i^-(\tau_k) = \hat{\rho}_i^+(\tau_k) = 0. \quad (33)$$

Now, perform the correction in our estimation by taking intersection of the box-sets (26) and (27):

$$\big\{\rho \in \mathbf{R}_+^N \mid \rho_i^-(\tau_k) \le \rho_i \le \rho_i^+(\tau_k),\ i = 1..N\big\} \cap \big\{\hat{\rho} \in \mathbf{R}_+^N \mid \hat{\rho}_i^-(\tau_k) \le \hat{\rho} \le \hat{\rho}_i^+(\tau_k),\ i = 1..N\big\}.$$

If this intersection is nonempty [7], update the bounds $\underline{\rho}(\tau_k)$ and $\overline{\rho}(\tau_k)$:

$$\underline{\rho}(\tau_k) = \begin{pmatrix} \max(0, \hat{\rho}_1^-(\tau_k), \min(\rho_1^-(\tau_k), \rho_1^{j-})) \\ \vdots \\ \max(0, \hat{\rho}_N^-(\tau_k), \min(\rho_N^-(\tau_k), \rho_N^{j-})) \end{pmatrix}, \quad (34)$$

$$\overline{\rho}(\tau_k) = \begin{pmatrix} \max(0, \min(\hat{\rho}_1^+(\tau_k), \rho_1^+(\tau_k), \rho_1^{j+})) \\ \vdots \\ \max(0, \min(\hat{\rho}_N^+(\tau_k), \rho_N^+(\tau_k), \rho_N^{j+})) \end{pmatrix}. \quad (35)$$

Otherwise, set

$$\underline{\rho}(\tau_k) = \min(\hat{\rho}_i^-(\tau_k), \rho_i^{j-}), \quad (36)$$

$$\overline{\rho}(\tau_k) = \min(\hat{\rho}_i^+(\tau_k), \rho_i^{j+}) \quad (37)$$

for $i = 1..N$.

4. If $k < K$, set $k = k + 1$, and repeat steps **2**, **3** and **4**.

Following this procedure we get the estimate of the state $\rho(t)$ at every time instant $t \in [0, T]$:

$$\rho^-(t) \le \rho(t) \le \rho^+(t).$$

6. APPLICATION: I-210 WEST

Chosen for simulation was the 14 mile segment of I-210 West freeway in Southern California, between Vernon Ave. (post mile (PM) 38.97) and I-210/I-710 split (PM 25.16). This freeway segment was divided into 40 cells according to the division rule from Section 2. PeMS data [7] was used to compute fundamental diagrams and split ratios, and to generate on-ramp demand profiles. CTMSIM [3] was used to run simulation.
The I-210 West traffic was simulated for six hours — from

[6] Information about the initial state may come from the previous estimation.

[7] In theory it must be nonempty, otherwise it would mean that wrong assumptions on the range of uncertainty in capacity or demand, or measurement noise, were made.

5.30 to 11.30 am with simulation time step 10 seconds, and on-ramp demand for 04/12/2006 coming from PeMS with 5 minute sampling period. The day was chosen because of high reliability of PeMS data due to good detector health and almost perfect match of CTMSIM simulation result with the PeMS measurements for that day. The time interval corresponds to morning rush hour.

The ±3% uncertainty in capacity and ±2% uncertainty in demand were introduced, and random values within the uncertainty intervals were chosen and fixed. Then, the density values were obtained from the simulation with these fixed random values. The corrections from flow and velocity measurements occured every 5 minutes, with the measurement data coming from PeMS for those cells, for which detector data was available, and from the original simulation with fixed fundamental diagrams and exact demands for all other cells. It was assumed that the actual flow and velocity values lie within ±2% of the measurement readings [8]. For the "measurements" obtained directly from simulation, the noise was artificially introduced.

Simulation with uncertainty and noisy measurements produced lower and upper bounds for the density along the investigated freeway segment. Fig. 5 shows the plot of the lower (green) and upper (red) density bounds together with the actual density (black) in one of the cells [9]. These lower and upper bounds are the results of the described estimation algorithm, and in reality they will be the only available data for the traffic responsive control algorithms. The "actual density", nonexistent in reality, comes from the simulation with fixed capacities and demands, whose values were randomly chosen within given uncertainty range.

Fig. 6 compares the density interval sizes coming only from the measurements (magenta) with the density interval sizes resulting from the intersection of the measurements and the CTM trajectory bounds (blue) obtained every 5 minutes. The smaller is the time between corrections, the smaller is the difference between the interval sizes and the smaller are the intervals themselves. Similar plots can be produced for other cells.

In the real Traffic Management Center application, CTM can provide projection of the state into the near future — the next 10-15 minutes, while being corrected with the measurement data, say, every 5 minutes.

Appendix A. INTERVAL ARITHMETIC

For real numbers $\underline{a}$, $\overline{a}$, $\underline{b}$ and $\overline{b}$, such that $\underline{a} \le \overline{a}$ and $\underline{b} \le \overline{b}$ define intervals $A = [\underline{a}, \overline{a}]$ and $B = [\underline{b}, \overline{b}]$, and the following operations.

Addition of two intervals.

$$A + B = \{x + y : \ x \in A, \ y \in B\} = [\underline{a} + \underline{b}, \overline{a} + \overline{b}]. \quad \text{(A.1)}$$

[8] The uncertainty and noise range was chosen arbitrarily for the sake of experiment.

[9] cell 34 between Hill Ave. off- and on-ramps (from PM 27 to PM 26.55).

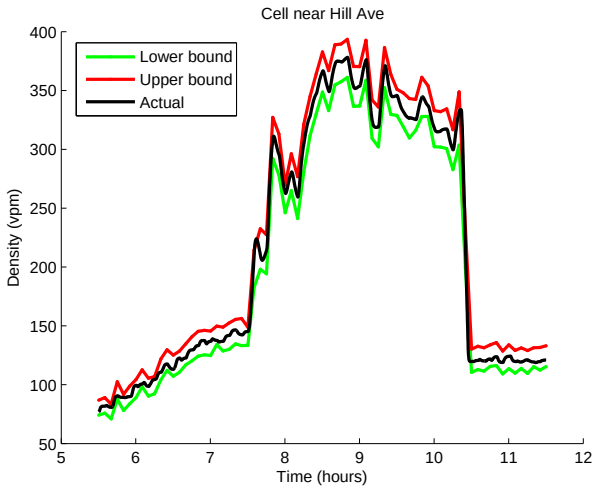

Fig. 5. Actual density with its lower and upper bounds.

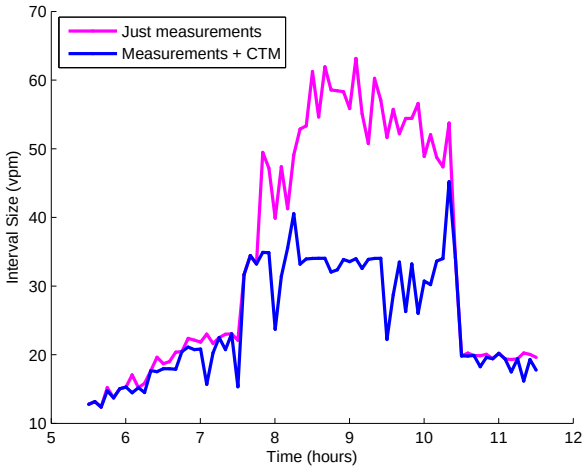

Fig. 6. Estimation intervals.

Negative of an interval.

$$-A = \{-x : \ x \in A\} = [-\overline{a}, -\underline{a}]. \quad \text{(A.2)}$$

Difference of two intervals.

$$A - B = A + (-B) = \{x - y : \ x \in A, \ y \in B\} = [\underline{a} - \overline{b}, \overline{a} - \underline{b}]. \quad \text{(A.3)}$$

Reciprocal of an interval.

$$1/A = \{1/x : \ x \in A\} = [1/\overline{a}, 1/\underline{a}], \quad \text{(A.4)}$$

which makes sense only if $\underline{a} > 0$ or $\overline{a} < 0$.

Product of two intervals.

$$AB = \{xy : \ x \in A, \ y \in B\} = [\underline{(ab)}, \overline{(ab)}], \quad \text{(A.5)}$$

where

$$\underline{(ab)} = \min(\underline{a}\underline{b}, \underline{a}\overline{b}, \overline{a}\underline{b}, \overline{a}\overline{b}) \quad \text{(A.6)}$$

$$\overline{(ab)} = \max(\underline{a}\underline{b}, \underline{a}\overline{b}, \overline{a}\underline{b}, \overline{a}\overline{b}) \quad \text{(A.7)}$$

Quotient of two intervals.

$$A/B = A(1/B) = \{x/y : \ x \in A, \ y \in B\}. \tag{A.8}$$

For $\underline{a} \geq 0$ and $\underline{b} \geq 0$,

$$A/B = [\underline{a}/\overline{b}, \overline{a}/\underline{b}]. \tag{A.9}$$

REFERENCES

[1] C. F. Daganzo. The cell transmission model: A dynamic representation of highway traffic consistent with the hydrodynamic theory. *Transportation Research, B*, 28(4):269–287, 1994.

[2] G. Gomes, R. Horowitz, A. A. Kurzhanskiy, J. Kwon, and P. Varaiya. Behavior of the Cell Transmission Model and Effectiveness of Ramp Metering. *Transportation Research, C*, 16(4):485–513, 2008.

[3] A. A. Kurzhanskiy and P. Varaiya. CTMSIM — An Interactive Macroscopic Traffic Simulator for MATLAB. 2008. Online: http://path.berkeley.edu/topl/docs.html.

[4] W. H. Lin. Spillovers, merging traffic and the morning commute. *Proceedings of the 4th IEEE Intelligent Transportation Systems Conference, Oakland, CA*, 2001.

[5] L. Munõz, X. Sun, R. Horowitz, and L. Alvarez. Traffic density estimation with the cell transmission model. *Proceedings of the 2003 American Control Conference*, pages 3750–3755, 2003.

[6] I. Okutani and Y. J. Stephanedes. Dynamic prediction of traffic volume through kalman filtering theory. *Transportation Research, B*, 18:1–11, 1984.

[7] Performance Measurement System (PeMS). http://pems.eecs.berkeley.edu.

[8] B. L. Smith, B. M. Williams, and R. K. Oswald. Comparison of parametric and nonparametric models for traffic flow forcasting. *Transportation Research, C*, 10:303–321, 2002.